Acta Geophysica (2019) 67:1319–1327
https://doi.org/10.1007/s11600-019-00339-6

RESEARCH ARTICLE - APPLIED GEOPHYSICS

On application of fractal magnetization in Curie depth estimation from magnetic anomalies

Chun-Feng Li[1,2] · **Duo Zhou**[1] · **Jian Wang**[3]

Received: 16 April 2019 / Accepted: 1 August 2019 / Published online: 10 August 2019

Abstract

As an independent geothermal proxy, the Curie-point depth has important geodynamic implications, but its estimation from magnetic anomalies requires an understanding of the spatial correlation of source magnetization, mathematically characterized by a fractal exponent. In this paper, we show that fractal exponent and Curie depth are so strongly inter-connected that attempts to simultaneous or iterative estimation of both of them often turn out to be futile. In cases of true large Curie depths, the iterative "de-fractal" method has a tendency of overcorrecting fractal exponents and thereby producing erroneously small Curie depths and smearing out true geological trends. While true fractal exponent can no way be constant over a large area, a regionally fixed fractal exponent is better than any mathematical treatments that are beyond the limit of data resolution and the underlying physics.

Keywords Curie depth · Geothermal structure · Heat flow · Fractal magnetization · Magnetic anomalies · Inversion · North America

Introduction

A wide variety of spectral techniques has been proposed to detect the depth to the bottom of the magnetic layer of the lithosphere from near-surface (or sometimes satellite) magnetic anomalies. This is also coined the Curie-point depth, where the temperature reaches the Curie point and rocks lose their ferromagnetism. Curie depths reflect deep thermal structure of the lithosphere assuming that the Curie temperature can be restricted to a narrow range (520–580 °C) for different mineralogy (Friedman et al. 2014). Curie temperatures decrease linearly with an increasing Ti content for natural terrestrial titanomagnetites (O'Reilly 1984), which are chemically stable at crust and upper mantle temperatures/pressures (Sauerzapf et al. 2008).

Among various techniques of detecting Curie depths, the linearized stepwise centroid method (Okubo et al. 1985; Tanaka et al. 1999), and its various extensions to fractal magnetization (Bansal et al. 2011; Li et al. 2009, 2010, 2013; Salem et al. 2014; Wang and Li 2015; Ravat et al. 2016), are theoretically simple but computationally stable. The reasoning behind this technique is simple; rather than seeking to directly estimate the Curie depth from nonlinear fitting between calculated and observed spectra of magnetic anomalies, Curie depth can be estimated indirectly from relatively easy linear inversion of the depths to the top and centroid of the magnetic layer, which are shallower than the magnetic bottom (Curie depth) and thereby more tractable computationally.

Curie depths are independent of Moho depths (or crustal thickness) and shallow radiogenic heat production, because the Moho is a lithological boundary, and radiogenic heat production decreases with depth (Turcotte and Schubert 2002), to have minimal effects at the Curie depth.

Examining amplitude (or power) spectra of magnetic anomalies offers by far the most valid and efficient means of estimating Curie depths over a large region. There are also geothermal methods based on the temperature-depth

✉ Chun-Feng Li
cfli@zju.edu.cn

[1] Department of Marine Sciences, Zhejiang University, Zhoushan 316021, China

[2] Laboratory for Marine Mineral Resources, Qingdao National Laboratory for Marine Science and Technology, Qingdao 266237, China

[3] Key Laboratory of Crustal Dynamics, Institute of Crustal Dynamics, China Earthquake Administration, Beijing 100085, China

relationship (Lachenbruch 1968; Negi et al. 1987). Curie depth can be correlated with surface heat flow (Li et al. 2010, 2017), and thereby is a good proxy to lithospheric thermal structure, particularly where heat flow measurements are sparse and hydrothermal activities could prevail (e.g., Li et al. 2017). Curie depths have been successfully applied to infer thermal evolution of oceanic lithosphere, global heat loss, lithospheric thermal conductivity, and regional geodynamics (e.g., Bansal et al. 2011; Li et al. 2009, 2010, 2013; Salem et al. 2014; Ravat et al. 2016; Wang and Li 2015), and to correlate with regional magmatism and seismicity (Tanaka and Ishikawa 2002, 2005; Manea and Manea 2011; Wang and Li 2015; Wang et al. 2016).

Despite these important applications, there are many caveats in estimating Curie-point depth, particularly in the application of fractal exponent of source magnetization. This paper is to clarify some of the confusions in applying fractal exponent in Curie depth estimation and outline the pitfalls that should be avoided in future applications.

Numerical backgrounds

Three-dimensional source magnetizations are spatially correlated and can be characterized by a scaling law.

$$\phi_M\left(k_x, k_y, k_z\right) \propto k^{-\beta_{3\mathrm{D}}^p} \tag{1}$$

in which $\beta_{3\mathrm{D}}^p$ is the fractal exponent and the superscript p refers to the definition for power spectrum, $\phi_M\left(k_x, k_y, k_z\right)$ is the 3D power spectrum of the magnetization, k_x, k_y and k_z are wavenumbers in x, y, and z directions, respectively, and their Euclidean norm $k = \sqrt{k_x^2 + k_y^2 + k_z^2}$.

Curie depths are dependent on wavenumber (or wavelength) distribution of magnetic anomalies, because the deeper the base of the magnetic layer, the more present are longer wavelength components. Theoretically, the radially averaged power (or amplitude) spectrum of total-field magnetic anomalies $A_{\Delta T}$ is linked to the spectrum of the magnetization and can be represented as a function of depths to the bottom (Z_b) and top (Z_t) of the magnetic layer, and the fractal exponent (Maus et al. 1997; Bouligand et al. 2009; Blakely 1995; Li et al. 2009).

To estimate Curie depths based on spectral methods, magnetic anomalies are interpolated and gridded and then divided into overlapping windows. Within each window, a radially averaged amplitude (or power) spectrum is calculated, from which a Curie depth is estimated from fitting the calculated spectrum to the theoretical models of Blakely (1995) or Maus et al. (1997). This windowing scheme can be skipped using wavelet transform (Gaudreau et al. 2019).

On the assumption of constant fractal exponent

In general, the fractal exponent of magnetization (named α in Ravat et al. 2016 in 2D, or β in 3D in many other papers, e.g., Bouligand et al. 2009; Li et al. 2013) is not known. In order to keep the inversion result stable and manageable, the fractal exponent is often assumed to be a known constant in a study area. Of course, it is unlikely that fractal exponent keeps constant across a large area due to the differing magnetic source characteristics. Undoubtedly, any method for Curie depth estimation is biased by the lack of knowledge of the fractal exponent (Audet and Gosselin 2019), or by using a single fractal exponent. Previous attempts have been made to estimate the fractal exponent $\left(\beta_{3\mathrm{D}}^p\right)$ simultaneously with the depths to the top and bottom (Z_b, Z_t) from magnetic anomalies based on a nonlinear inversion scheme, but it turned out to be very difficult as these parameters are strongly inter-dependent (Ravat et al. 2007; Li et al. 2010). The best constraints on estimated Curie depths and the fractal exponent are from known geology, such as shallow geotherms associated with mid-ocean ridges and active volcanoes (Li et al. 2013, 2017). Alternatively, Mather and Fullea (2019) combined independent geophysical data with magnetic anomaly data in a probabilistic framework to constrain geotherms. Gaudreau et al. (2019) determine the fractal exponent a posteriori by comparing Monte Carlo simulations of predicted heat flow with observed heat flow in various regions.

One of the strategies is a stepwise linearized inversion for Z_t at intermediate to high wavenumbers and the depth to the centroid (Z_o) at small wavenumbers (Tanaka et al. 1999), assuming a regionally constant fractal exponent. This constant assumption is found effective and valid in previous regional and global studies, giving useful geothermal information conformable to real geology (e.g., Bouligand et al. 2009; Li et al. 2013, 2017).

Li et al. (2009, 2013) applied the centroid method assuming a constant fractal exponent. Bouligand et al. (2009) applied a one-step nonlinear fitting in their western North America study, also assuming a constant fractal exponent. Uncertainties are involved in selecting the best fitting intervals in the two-step linearized method. However, with fixed fitting intervals, Li et al. (2010) showed that the two-step centroid method can give more stable Curie depth results than the one-step nonlinear simultaneous inversion.

On the "de-fractal" method

Salem et al. (2014) and Ravat et al. (2016) argued that they could test a set of fractal exponents β by visual inspection of fit between observed and modeled power spectra,

and found the optimal β for correcting observed spectrum before estimating Curie depth (Fig. 1). They coined their methods "de-fractal" spectral depth determination, which involves forward modeling to fit spectral peaks, and numerical iteration and visual inspection to select β. These iterative procedures are time-consuming.

Correction of the spatially correlated magnetization has been practiced in many other studies (e.g., Bouligand et al. 2009; Bansal et al. 2011; Li et al. 2013). The terminology "de-fractal" is unnecessary for the following reasons.

(1) Magnetization is universally fractal, i.e., spatially correlated. Fitting an observed spectrum with a theoretical model can be done without "de-fractal" because the theoretical models can handle fractal magnetization neatly (Blakely 1995; Maus et al. 1997; Li et al. 2013).
(2) "De-fractal" is operated only in a relative sense because two-dimensional spatially uncorrelated magnetization can be spatially correlated in three dimensions. "De-fractal" is meaningful only when the dimension of the reference space is identified. Randomness (uncorrelation) is just a special form of fractal.

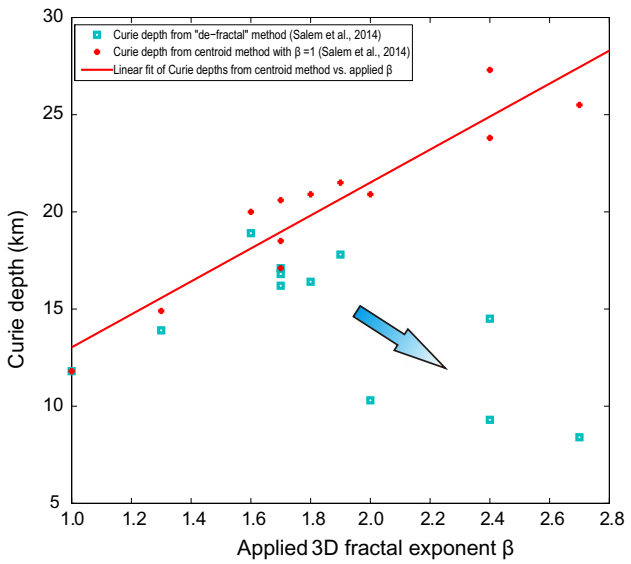

Fig. 1 A positive correlation is noticed between Curie depths estimated with a constant fractal exponent (red cross) and applied fractal exponents in the "de-fractal" method in the central Red Sea. In other words, the "de-fractal" method tends to apply a larger fractal exponent where the Curie depths could be larger if keeping a constant fractal exponent, and consequently gives smaller Curie depth estimates (data in blue squares). This over-correlation tendency (marked by the blue arrow) leads to systematic computational errors in the "de-fractal" method. The straight line is from least square fitting. Depths are below sea level from Salem et al. (2014)

There are other three more important issues in both the visual (Salem et al. 2014) and semiautomatic (Ravat et al. 2016) "de-fractal" method.

(1) The first is the often subjective and random selection of fitting intervals and wavenumbers of spectrum. Theoretical and numerical models suggested that the fitting intervals for estimating the centroid depth should be fixed to the smallest wavenumbers, unless a peak occurs in the fractal-corrected and wavenumber-scaled spectrum, which is likely due to windowing (Li et al. 2013). In the case a peak occurs, points to the smallest wavenumber side of the spectral peak should be simply ignored in data fitting (Li et al. 2013). While estimating Curie depth from the steepest segment is theoretically sound (Li et al. 2013), fitting just on the steepest segment of the spectrum with only 2 or 3 controlling points is prone to large fitting uncertainties.
(2) The second major uncertainty rests upon changing fractal exponent β from window to window (Fig. 1). In each iteration, a modeled power spectrum is produced to match with the observed one, and when an acceptable visual fit is found with a particular fractal exponent, that fractal exponent is chosen as an a priori input for the next step of Curie depth estimation (Ravat et al. 2016). Identical to the number of unknowns in the inversion, an equal number of parameters are needed in the forward modeling of the "de-fractal" scheme. In other words, forward modeling is dependent not just on fractal exponent, but also on depths to the magnetic layer, which are also unknowns. A large Curie depth will induce magnetic anomalies with more long-wavelength signals, as if from a highly correlated magnetization of large fractal exponent, which also equivalently induces more long-wavelength magnetic signals. The reverse is also true. There is essentially no work-around to know the best-fit fractal exponent. Therefore, the "de-fractal" method is circular and does not have anything internal to the Curie depth calculation to tie results to. Consequently, the "de-fractal" method results in low resolution and likely high error (Fig. 1).

Changing fractal exponents β that are not well constrained from window to window introduces additional error, because this will smear out Curie depth anomalies associated with true geological features. Although the "de-fractal" method appears to give a mechanism to constrain the fractal exponent β in an iterative way, in reality it can do more harm than help.

By plotting Curie depths from Table 2 of Salem et al. (2014), who applied the "de-fractal" method, we further demonstrate that their applied fractal exponent is strongly correlated with Curie depth estimated

with a constant fractal exponent (Fig. 1). The larger the Curie depth, the larger were their applied fractal exponents for spectral correction, and the smaller were their finally estimated Curie depths. The consequence is that, wherever there are large Curie depths, this "de-fractal" operation tends to systematically pick large fractal exponents and obtain small Curie depths with overcorrection. This can distort the final Curie depth map. In other words, the "de-fractal" method can mistakenly interpret large Curie depths as from large fractal exponents. The best and likely the only constraints on estimated Curie depths are from known geology, such as shallow geotherms associated with mid-ocean ridges and active volcanoes (Li et al. 2013, 2017), or from other independent geophysical measurements such as heat flow (e.g., Mather and Fullea 2019; Gaudreau et al. 2019), but not from some calculated mathematical operations. With a tendency of overcorrection and almost a random selection of fractal exponent that is strongly dependent on the correlation of the treated magnetic anomalies (Fig. 1), the "de-fractal" method cannot map, in a consistent and systematic manner, true geological units of similar scaling in spatial magnetization.

(3) The "de-fractal" method compensates for the fractal parameter of the magnetic anomaly field such that a spectral peak is formed. Whether a peak could occur or not is not solely dependent on the fractal parameter, but also on the Curie depth and applied window size (Li et al. 2010, 2013). For the same fractal parameter, shallow Curie depths can also give spectral peaks. Occurrence of a spectral peak is not a correct criterion for judging the fractal exponent of the underlying magnetization.

On the detection limit

With a 500 km window length and the recommended wavenumber range of Li et al. (2013), Ravat et al. (2016) compared their results from the "de-fractal" method with those of Li et al. (2013), who applied an automatic fractal centroid method. Ravat et al. (2016) showed that they can get even more accurate Curie depth estimate with the smallest error bar for the deepest 40 km depth test.

It is all known in geophysics that the deeper the target, the more uncertainties and difficulties are in geophysical inversion. Ravat et al. (2016) did not state how they obtained the Curie depths from the method of Li et al. (2013) and showed neither numerical/synthetic models (like Fig. 4 of Li et al. 2013), upon which these tests were performed, nor power spectra for fitting. Numerical and synthetic models of 3D magnetization and corresponding magnetic anomalies and power spectra are needed to validate their argument. A regional map of their applied fractal exponents should also be presented to aid in the interpretation and assessment of their results, because the degree of correction affects the estimated Curie depths.

Ravat et al. (2016) showed that they estimated the centroid depth directly from fitting the spectrum itself, not from the required wavenumber-scaled spectrum, because the vertical axes of these two figures are labeled with "Annular Average of ln of Amplitude (nT)." This might be just a typo, and they stated in the caption that the calculation was based on wavenumber-scaled spectrum. However, the labeled unit "nT" is misleading, because the amplitude here is the spectral strength at certain wavenumbers, surely no longer the original magnetic anomaly amplitudes with the unit "nT." Furthermore, using only 2 or 3 controlling points for linear regression for the steepest segment of the spectrum introduces large uncertainties and inconsistencies.

Numerical synthetic modeling with known and fixed fractal exponents showed that, with a set of input Curie depths of 10.0, 20.0, 30.0 and 40.0 km, the inverted depths are 9.5, 13.1, 26.2, and 35.0 km, respectively (Li et al. 2013). Plotting this early result of synthetic test on Fig. A2 of Ravat et al. (2016) shows that the two-step linearized method captures the overall trend of input Curie depth, but tends to underestimate it (Fig. 2). There are several reasons behind this underestimation.

Firstly, magnetic anomalies from deeper sources are more attenuated by the Earth filter, and we have to deal with a narrow band of long wavelengths and work on very small wavenumbers containing the centroid depth information. Secondly, we apply windowing in practice on magnetic anomalies, whereas the mathematical models assume infinite horizontal extension (Blakely 1995; Maus et al. 1997). Thirdly, the linearized centroid technique is itself based on an approximation of the nonlinear system.

These theoretical and practical limitations apply to all Curie depth inversion techniques. We can partly circumvent these issues of underestimation by choosing a smaller fractal exponent in spectrum correction. Nonlinear inversion can be tested on synthetic models to expect larger, albeit unstable, Curie depths (Li et al. 2010). However, there is a mutual dependence of depths to the top and bottom of the magnetic layer in the nonlinear inversion, and solutions can be non-unique. In addition, the nonlinear method also requires data fitting only at the very narrow-banded low-wavenumber portion of the spectrum, producing highly fluctuating results with just a few controlling data points (Li et al. 2010).

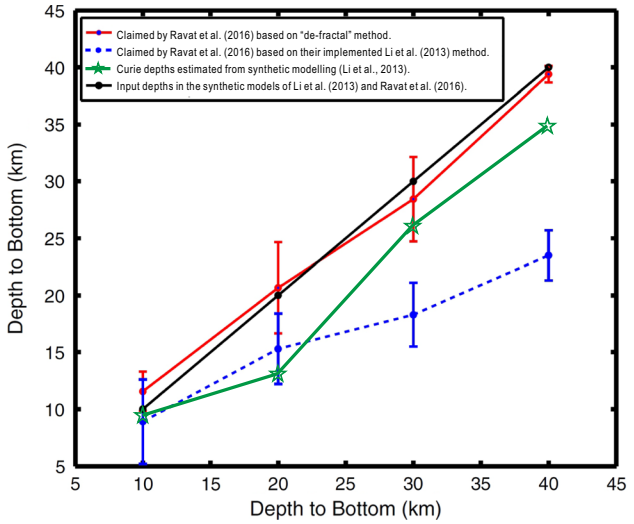

Fig. 2 Comparison of numerical results from the "de-fractal" method with a 500 km window by Ravat et al. (2016), from Li et al. (2013) fractal correction centroid method implemented by Ravat et al. (2016), and from synthetic modeling of 3D magnetization of Li et al. (2013)

Comparison between known Curie depth results in North America

We here make a comparison among published Curie depth results in the Northern Colorado–Wyoming Craton area (Fig. 3; Table 1). Bouligand et al. (2009) mapped Curie depths in the western USA with a fractal magnetization model based on nonlinear inversion (Fig. 3d). Based on the linearized centroid method, Li et al. (2017) developed a global Curie depth model (GCDM), using nearly the same window size range and fractal exponent as Bouligand et al. (2009), but a different magnetic dataset of lower resolution (Maus et al. 2009) (Table 1). Part of the GCDM is shown here for comparison (Fig. 3b). One can easily notice that these two maps show very similar features. The Yellowstone hotspot trail, the northern and southern Rocky Mountains, and a large part of Colorado Plateau have smaller Curie depths. There is also a belt of small Curie depths to the east margin of the study area in the Great Plains. By contrast, the Wyoming Craton shows mostly large Curie depths (Fig. 3b, d). It can also be seen that, as expected and mentioned above, nonlinear inversion resulted in more fluctuating estimates (Fig. 3d) than the centroid method (Fig. 3b), producing many points shallower than 10 km and deeper than 30 km. The apparent higher resolution of Fig. 3d is mostly likely due to the higher resolution of the North America magnetic grid (NAMAG 2002) applied by Bouligand et al. (2009), as well as to more fluctuating nonlinear estimates.

Also based on this high-resolution NAMAG, Wang and Li (2015) examined Curie depths with smaller windows in western North America (Fig. 3c). Figure 3b, c is from different data sources of different resolution and from applying different window sizes, and thereby some differences in resolution and values between them are expected. Both the high-resolution input data and smaller window size gave high resolution in the mapped Curie depths that conform to real geology (Fig. 3c). The central eroded and rifted drainage basin of the Colorado River in the Colorado Plateau shows smaller Curie depths (Fig. 3c), which could indicate thermal rejuvenation at depth. The two areas of smaller Curie depths of the Snake River Plain and the northern Rocky Mountains can be distinguished from each other on the high-resolution result. Overall, these three Curie depth results (Fig. 3b–d) show similar features that are consistent to known geology and can be correlated with surface heat flow (Fig. 3f).

The Yellowstone hotspot turns out not to be a good control point on Curie depth because presently it has very strong hydrothermal activity (Bryan 2008), which can lower the regional deep temperature considerably, like in young oceanic lithospheres. Li and Wang (2018) have shown that strong hydrothermal activity along the fast spreading mid-ocean ridge can lower the mantle temperature and increase the Curie depth. Our reasoning of strong hydrothermal influence on the deep temperature is also drawn from the discrepancy between heat flow (Fig. 3f) and Curie depth (Fig. 3b–d) along the Snake River Plain. Instead of in the central Snake River Plain of the smallest Curie depths, the highest heat flow is found in the surrounding uplifted shoulders of the plain, where fractures, evident on the topographic map (Fig. 1), may drain deep hot hydrothermal fluids.

Again, one cannot guarantee that Curie depth estimation using different window sizes and data of different resolution can give identical result at the same single location, because different window sizes focus on different anomalies, and different data resolution focuses on different wavelengths. Nonetheless, regional features should remain the same and should be captured, such as the shallow Curie depths of the Yellowstone hotspot trail (Snake River Plain, Fig. 3).

The "de-fractal" result (Fig. 3e) is quite different from the other three, neither revealing the large Curie depth contrast between the Colorado Plateau and the Wyoming Craton, nor showing small Curie depth zones associated with the Snake River Plain and the northern Rocky Mountains. Instead, Fig. 3e shows smaller Curie depths to the east of the southern Rocky Mountains, which are not present on other three maps. Without knowing areal distribution of the fractal exponents, it is very difficult to assess the "de-fractal" result. Surface heat flow (Fig. 3f) has better correlations to the Curie depths of Bouligand et al. (2009) and Li et al. (2017) than to the "de-fractal" result (Fig. 3e). This demonstrates again that the "de-fractal" method, with variable fractal exponents that cannot be accurately determined and are strongly correlated with Curie depths themselves (Fig. 1),

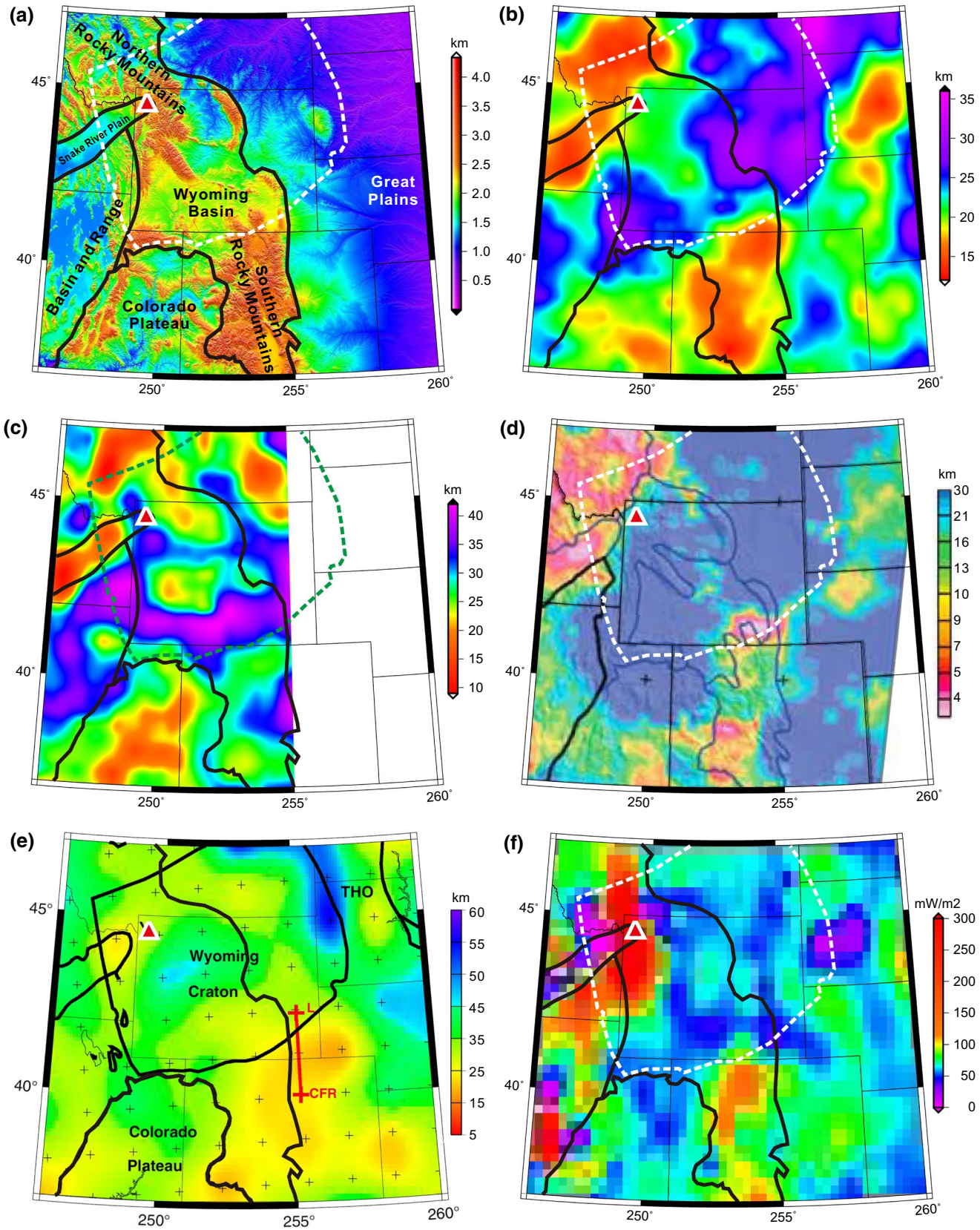
(a)
Northern Rocky Mountains
Snake River Plain
Wyoming Basin
Great Plains
Basin and Range
Rocky Mountains
Southern
Colorado Plateau
km
4.0
3.5
3.0
2.5
2.0
1.5
1.0
0.5
45°
40°
250°
255°
260°
(b)
km
35
30
25
20
15
(c)
km
40
35
30
25
20
15
10
(d)
km
30
21
16
13
10
9
7
5
4
(e)
THO
Wyoming
Craton
L
CFR
Colorado
Plateau
km
60
55
50
45
35
25
15
5
(f)
mW/m2
300
250
200
150
100
50
0

◂**Fig. 3** Comparison between known Curie depth results in the western North America. **a** Topography of the study area. The white dashed line outlines the Wyoming Craton shown in Ravat et al. (2016). Thick black lines outline major tectonic units. The red triangle marks the Yellowstone hotspot. **b** Curie depths from the global reference Curie depth model (GCDM) of Li et al. (2017). **c** Curie depths from Wang and Li (2015). The green dashed line outlines the Wyoming Craton shown in Ravat et al. (2016). No Curie depths were obtained to the east of the 255° longitude line. **d** Curie depths from Bouligand et al. (2009). **e** Curie depths from the "de-fractal" method, and the black solid line outlines the Wyoming Craton (Ravat et al. 2016). **f** Surface heat flow gridded in a 30′ interval using the minimum curvature algorithm with tension (Briggs 1974) (heat flow data from the international heat flow commission database https://www.heatflow.und.edu/; last updated in January 2011). No preselection or preprocessing is done on the original raw heat flow data. Red line shows the location of a thermal property profile in Ravat et al. (2016). Data mapping is supported by GMT (Wessel and Smith 1995)

can smear out true geological features with distorted Curie depth maps.

Application of "de-fractal" Curie depths casts doubt on the derived geothermal result, which shows that Wyoming geotherm is hotter by ~ 200 °C at the Curie depth than the Decker et al. (1988) model. The Wyoming Craton shows largely low heat flow (Fig. 3f) and deep and heterogeneous Curie depths (Fig. 3b–d). The heterogeneity in the Wyoming Craton stems from late tectonism, which has already divided it into different subunits of contrasting topography (Fig. 3a) and heat flow (Fig. 3f). Strictly, the Wyoming Craton can no longer be regarded as a typical craton. The anomalously hotter and uniform geotherm of Ravat et al. (2016) is, in our opinion, due to their estimated shallow Curie isotherm, which makes no distinction of the Wyoming Craton on their Curie depth map (Fig. 3e).

A very large applied window size of 500.0 km may also contribute to this loss of information. Ideally, the long-wavelength components carrying the information of Curie depth can be best captured by using very large windows, but the incorporation of fractal exponent, which deals with the wide (correlated) but shallow anomalies, partially relieves this requirement. Increasing window size does not appreciably increase calculated Curie depth, but merely leads to a low resolution (Li et al. 2010, 2013). This is because the extra information we can gain at the smallest wavenumbers (or longest wavelengths) is rather minimal (Fig. 4); one can never approach the theoretically required scale of infinity by just attempting to increase the window length by several hundred kilometers. The strong averaging effect of large windows can decrease, not increase, locally large Curie depths, for example, those associated with a cold accretionary wedge. Features smaller than the chosen window size will not be properly imaged, because normally only one Curie depth is estimated in each window, and the small feature contributes only partially to the radially averaged spectrum in that window. It can also be seen that most of the "de-fractal" Curie depths in the study area are between 15 and 40 km, although the color bar shows much larger values (Fig. 3e), and are not appreciably larger than those from using the centroid method (Fig. 3b, c). A Curie depth comparison between using a larger window size (Fig. 3b) and a smaller window sizes (Fig. 3c) also shows that a significantly large window size at 500.0 km is not necessary.

Conclusion

This paper intends to clarify that mathematical treatment beyond the limit of data resolution and the underlying physics could introduce additional errors to Curie depth estimation. Wherever there are true large Curie depths, the "de-fractal" method, by its very nature, has a tendency of overcorrecting fractal exponents and thereby producing small Curie depths and smearing out true geological trends.

For Curie depth estimation in a large area, the fractal exponent cannot be a constant, but it can be better fixed than variable but just loosely controlled purely by mathematical overtreatment. At long wavelengths containing primarily the Curie depth information, fractal exponents of source magnetizations are expected to be rather stable over a large area. Long-distance spatial correlation in source magnetization

Table 1 Comparison of parameters applied in four different Curie depth results

Author	Method	Window size (km)	3D fractal exponent β	Data source
Bouligand et al. (2009)	Nonlinear inversion	100.0 to 300.0	3.0	Magnetic anomaly map of North America (NAMAG 2002) and the state map of Nevada (Kucks et al. 2006)
Wang and Li (2015)	Centroid	80.0, 100.0 and 120.0	2.5	Magnetic anomaly map of North America (NAMAG 2002)
Li et al. (2017)	Centroid	98.8, 195.0, and 296.4	3.0	Earth Magnetic Anomaly Grid of 2′ resolution (EMAG2, Maus et al. 2009)
Ravat et al. (2016)	"De-fractal," based on centroid	500.0	Variable but unknown	Unknown

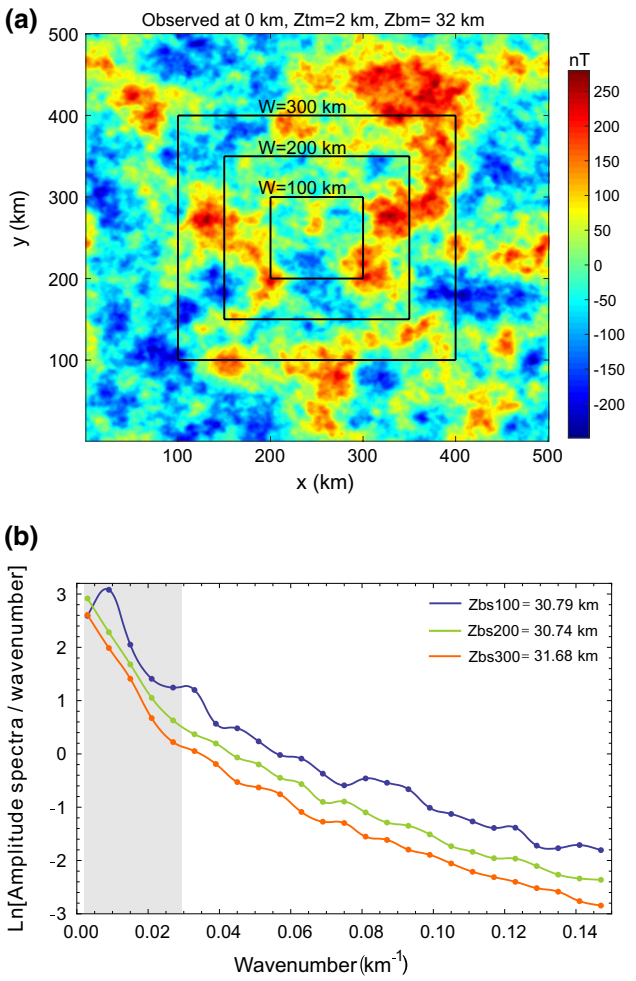

Fig. 4 Testing of window size effect on Curie depth estimation. **a** Magnetic anomalies calculated at the surface of the North Pole from a 3D synthetic fractal magnetization model. The magnetization has a Gaussian distribution with a mean value of 0 A/m and a standard deviation of 0.3 A/m. The fractal exponent, the top (*Z*tm) and bottom (*Z*bm) depths to the magnetic sources of the input model are taken as 3, 2 km and 32 km, respectively. Black squares depict the three window lengths of 100, 200 and 300 km. **b** Wavenumber-scaled radially averaged amplitude spectra of the synthetic magnetic anomalies using the three different window sizes shown in **a**. Estimated Curie depths indicate that increasing window size does not considerably lead to larger Curie depths. The gray shadow zone indicates where the centroid depths are estimated from linear regressions. The centroid depth predominates the Curie depth

is related to more regional geological features, whose geothermal conditions and source magnetizations are unlikely to alter swiftly in short distances or between two nearby windows. Therefore, a constant fractal exponent constrained by geology is preferred, when the true fractal exponent is not obtainable, over a method trying to vary the fractal exponents but in an overcorrection tendency.

Significantly large window lengths at ~ 500.0 km are not necessary for capturing large Curie depths. Normally using multiple window sizes ranging from tens of kilometers to 200.0 km is sufficient, and an average from these different windows can suppress random noise and increase the resolution of Curie depths. With magnetic anomalies of increasing resolutions to be available in the future, the calculated Curie depths should be improved, mostly from better calibrating the depths to the magnetic top in the intermediate to large wavenumbers. But since Curie depths are more dependent on long wavelengths, better data coverage is even more critical.

The linearized stepwise centroid method has proven to be stable and efficient, and gained more applications. In recent years, new techniques, such as Bayesian inversion (Mather and Fullea 2019; Audet and Gosselin 2019), multitaper spectral analysis (Audet and Gosselin 2019), and wavelet transform (Gaudreau et al. 2019), are being applied in Curie depth estimation. By statistically incorporating independent geological and geophysical constraints, the fractal exponent could be better estimated prior to the inversion of Curie depth. Ensemble-based approaches can produce probability distributions and provide greater confidence for the recovered parameters.

Acknowledgements This study is funded by National Natural Science Foundation of China (Grant Nos. 41776057, 41761134051, 41704086 and 91858213). Data mapping is supported by GMT (Wessel and Smith 1995). We thank anonymous reviewers for their critical but positive suggestions.

References

Audet P, Gosselin JM (2019) Curie depth estimation from magnetic anomaly data: a re-assessment using multitaper spectral analysis and Bayesian inference. Geophys J Int 218:494–507. https://doi.org/10.1093/gji/ggz166

Bansal AR, Gabriel G, Dimri VP, Krawczyk CM (2011) Estimation of depth to the bottom of magnetic sources by a modified centroid method for fractal distribution of sources: an application to aeromagnetic data in Germany. Geophysics 76:L11–L22. https://doi.org/10.1190/1.3560017

Blakely RJ (1995) Potential theory in gravity and magnetic applications. Cambridge University Press, Cambridge, pp 1–464

Bouligand C, Glen JMG, Blakely RJ (2009J) Mapping Curie temperature depth in the western United States with a fractal model for crustal magnetization. J Geophys Res 114:B11104. https://doi.org/10.1029/2009JB006494

Briggs IC (1974) Machine contouring using minimum curvature. Geophysics 9:39–48

Bryan TS (2008) The geysers of Yellowstone. University Press of Colorado, Niwot, pp 1–456

Decker ER, Heasler HP, Buelow KL, Baker KH, Hallin JS (1988) Significance of past and recent heat-flow and radioactivity studies in the Southern Rocky Mountains region. Colo Geol Soc Am Bull 100:1851–1885

Friedman SA, Feinberg JM, Ferré EC, Demory F, Martín-Hernández F, Conder JA, Rochette P (2014) Craton vs. rift uppermost mantle contributions to magnetic anomalies in the United States interior. Tectonophysics 624–625:15–23

Gaudreau É, Audet P, Schneider DA (2019) Mapping Curie depth across western Canada from a wavelet analysis of magnetic anomaly data. J Geophys Res 124:4365–4385. https://doi.org/10.1029/2018JB016726

Kucks RP, Hill PL, Ponce DA (2006) Nevada magnetic and gravity maps and data: a website for the distribution of data, U.S. geological survey data series, 234. https://pubs.usgs.gov/ds/2006/234. Accessed Aug 2017

Lachenbruch AH (1968) Preliminary geothermal model of the Sierra Nevada. J Geophys Res 73:6977–6988

Li C-F, Wang J (2018) Thermal structures of the Pacific lithosphere from magnetic anomaly inversion. Earth Planet Phys 2:52–66

Li C-F, Chen B, Zhou Z (2009) Deep crustal structures of eastern China and adjacent seas revealed by magnetic data. Sci China Ser D Earth Sci 52:984–993. https://doi.org/10.1007/s11430–009–0096-x

Li C-F, Shi XB, Zhou ZY, Li JB, Geng JH, Chen B (2010) Depths to the magnetic layer bottom in the South China Sea area and their tectonic implications. Geophys J Int 182:1229–1247. https://doi.org/10.1111/j.1365-246X.2010.04702.x

Li C-F, Wang J, Lin J, Wang T (2013G) Thermal evolution of the North Atlantic lithosphere: new constraints from magnetic anomaly inversion with a fractal magnetization model. Geochem Geophys Geosyst 14:5078–5105. https://doi.org/10.1002/2013GC004896

Li C-F, Lu Y, Wang J (2017) A global reference model of Curie-point depths based on EMAG2. Sci Rep 7:45129. https://doi.org/10.1038/srep45129

Manea M, Manea VC (2011) Curie point depth estimates and correlation with subduction in Mexico. Pure Appl Geophys 168:1489–1499

Mather B, Fullea J (2019) Constraining the geotherm beneath the British Isles from Bayesian inversion of Curie depth: integrated modelling of magnetic, geothermal, and seismic data. Solid Earth 10:839–850. https://doi.org/10.5194/se-2019-9

Maus S, Gordan D, Fairhead D (1997) Curie-temperature depth estimation using a self-similar magnetization model. Geophys J Int 129:163–168. https://doi.org/10.1111/j.1365-246X.1997.tb00945.x

Maus S, Barckhausen U, Berkenbosch H, Bournas N, Brozena J, Childers V, Dostaler F, Fairhead JD, Finn C, von Frese RRB, Gaina C, Golynsky S, Kucks R, Luhr H, Milligan P, Mogren S, Müller D, Olesen O, Pilkington M, Saltus R, Schreckenberger B, Thébault E, Caratori Tontini F (2009G) EMAG2: a 2-arc-minute resolution earth magnetic anomaly grid compiled from satellite, airborne and marine magnetic measurements. Geochem Geophys Geosyst 10:Q08005. https://doi.org/10.1029/2009GC002471

Negi JG, Agrawal PK, Pandey OP (1987) Large variation of Curie depth and lithospheric thickness beneath the Indian subcontinent and a case for magnetothermometry. Geophys J R Astr Soc 88:763–775

North American Magnetic Anomaly Group (NAMAG) (2002) Digital data grids for the magnetic anomaly map of North America, U.S. geological survey open file rep. 02–414. https://pubs.usgs.gov/of/2002/ofr-02-414/. Accessed Aug 2017

O'Reilly W (1984) Rock and mineral magnetism. Blackie Academy and Professor, London

Okubo Y, Graf RJ, Hansen RO, Fytikas M (1985) Curie point depths of the Island of Kyushu and surrounding areas, Japan. Geophysics 53:481–494. https://doi.org/10.1190/1.1441926

Ravat D, Pignatelli A, Nicolosi I, Chiappini M (2007) A study of spectral methods of estimating the depth to the bottom of magnetic sources from near-surface magnetic anomaly data. Geophys J Int 169:421–434

Ravat D, Morgan P, Lowry A (2016) Geotherms from the temperature-depth–constrained solutions of 1-D steady-state heat-flow equation. Geosphere 12:1187–1197. https://doi.org/10.1130/GES01235.1

Salem A, Green C, Ravat D, Singh KH, East P, Fairhead JD, Mogren S, Biegert E (2014) Depth to Curie temperature across the central Red Sea from magnetic data using the de-fractal method. Tectonophysics 624–625:75–86

Sauerzapf U, Lattard D, Burchard M, Engelmann R (2008) The titanomagnetite-ilmenite equilibrium: new experimental data and thermooxybarometric application to the crystallization of basic to intermediate rocks. J Petrol 49:1161–1185

Tanaka A, Ishikawa Y (2002) Temperature distribution and focal depth in the crust of the northeastern Japan. Earth Planets Space 54(11):1109–1113

Tanaka A, Ishikawa Y (2005) Crustal thermal regime inferred from magnetic anomaly data and its relationship to seismogenic layer thickness: the Japanese islands case study. Phys Earth Planet Int 152(4):257–266

Tanaka A, Okubo Y, Matsubayashi O (1999) Curie point depth based on spectrum analysis of the magnetic anomaly data in East and Southeast Asia. Tectonophysics 306:461–470. https://doi.org/10.1016/S0040-1951(99)00072-4

Turcotte DL, Schubert G (2002) Geodynamics. Cambridge University Press, New York

Wang J, Li C-F (2015) Crustal magmatism and lithospheric geothermal state of western North America and their implications for a magnetic mantle. Tectonophysics 638:112–125. https://doi.org/10.1016/j.tecto.2014.11.002

Wang J, Li CF, Lei JS, Zhang GW (2016) Relationship between seismicity and crustal thermal structure in North China. Acta Seismol Sin 38(4):618–631

Wessel P, Smith WHF (1995) New version of the generic mapping tools (GMT) version 3.0 released. Trans Am Geophys Union EOS 76:329